

Comparison of a Two- and Three-Dimensional Drift Model

S. E. S. Ferreira¹, M. S. Potgieter^{1,2} and R. A. Burger¹

¹Space Res. Unit, School of Physics, Potchefstroom University for CHE, 2520 Potchefstroom, South Africa

²International Space Science Institute, Hallerstrasse 6, CH-3012 Bern, Switzerland

Abstract

The modulation of galactic cosmic ray electrons in the heliosphere was used to compare solutions of a two- (2D) and a three-dimensional (3D) drift model, both developed by the Potchefstroom Modulation Group. These steady-state models are based on the numerical solution of Parker's transport equation and include the main modulation mechanisms; convection, diffusion, gradient, curvature and neutral sheet drifts. Examining computed electron spectra, with identical modulation parameters in both models, as a function of the heliospheric neutral sheet "tilt angle" yielded no qualitative differences and insignificant quantitative differences between the solutions of the 2D and 3D models. Taking into account the large amount of resources needed for the 3D model, the use of a 2D model for modulation studies is well justified.

1 Introduction

The modulation of galactic cosmic rays in the heliosphere is described successfully by Parker's (1965) transport equation (TPE). This TPE has been solved with increasing complexity over the years. However, to solve it numerically for three spatial dimensions (3D), a rigidity and a time-dependence is rather complex and has not yet been done successfully. By assuming an axisymmetric cosmic ray distribution one can neglect the equation's azimuthal dependence which leads to 2D models which have been used widely for modulation studies (le Roux & Potgieter, 1990). The main difficulty in 2D models is how to emulate the effect of the wavy heliospheric current sheet (HCS) because it cannot be done directly. This was done successfully for the first time by Potgieter & Moraal (1985). The technique was improved by Burger & Potgieter (1989). Hattingh (1993) developed a refined 2D model, which was called the WCS model, and more recently also a 3D model which includes an actual wavy HCS (Burger & Hattingh 1995, Hattingh 1998). This 3D model was compared carefully to the first 3D model developed by Kóta & Jokipii (1983) with excellent results. For a review and detail of the different models, see le Roux & Potgieter (1990), Hattingh & Burger (1995a,b), Burger & Hattingh (1995) and for an application of the 3D model, see Burger & Hattingh (1998).

An obvious next step was to compare the 2D and 3D models to establish how reliable the 2D models are, and to establish to what extent they can be used for modulation studies. This was done by Hattingh (1998) for cosmic ray protons and it was found that the agreement between the 3D and the 2D WCS model varied between good to excellent. At Earth, the largest variation of ~16% in the ratio of the two sets of solutions was found at low rigidities for a "tilt angle" $\alpha = 20^\circ$ during an $A < 0$ (e.g. ~1980 to ~1990) solar polarity cycle. At 60 AU, the largest variation was ~26% at low energies during the $A < 0$ cycle. This comparative study was continued by Ferreira (1999) who concentrated on the modulation of cosmic ray electrons in the heliosphere because electrons may have a different diffusion tensor than protons, experience less adiabatic energy losses than protons at energies of interest to modulation, and for which drifts become less significant with decreasing energy. This paper reports on the comparative study of the 2D and 3D models using electron modulation, with emphasis on the "tilt angle" dependence because the computation of the wavy HCS and its effects on modulation are the important difference between the 2D and 3D numerical models.

2 The Modulation Model

A short description of the 2D WCS model is given by Ferreira et al. (SH3.1.14) with detail given by Burger & Hattingh (1995). The 3D model is based on the numerical solution of Parker's (1965) equation:

$$\frac{\partial f}{\partial t} = -(\mathbf{V} + \langle \mathbf{v}_D \rangle) \cdot \nabla f + \nabla \cdot (\mathbf{K}_s \cdot \nabla f) + \frac{1}{3} (\nabla \cdot \mathbf{V}) \frac{\partial f}{\partial \ln P}, \quad (1)$$

where \mathbf{V} is the solar wind velocity and $f(\mathbf{r}, P, t)$ is the CR distribution function where P is rigidity, \mathbf{r} is position, and t is time. The symmetric part of the tensor K_s consists of a parallel diffusion coefficient (K_{\parallel}) and a perpendicular diffusion coefficient (K_{\perp}). The antisymmetric element K_A describes gradient and curvature drifts in the large scale heliospheric magnetic field (HMF). The pitch angle averaged guiding centre drift velocity for a near isotropic CR distribution is given by $\langle \mathbf{v}_d \rangle = \nabla \times [h(\mathbf{r})K_A \mathbf{e}_B]$ with $\mathbf{e}_B = \mathbf{B}/B$, where B is the magnitude of the background HMF and $h(\mathbf{r})$, a transition function which varies from 1 to -1 across the HCS and is zero in the HCS. This transition function modifies K_A across the wavy HCS which is positioned at $\theta' = \frac{\pi}{2} + \alpha \sin\left(\phi + r \frac{\Omega}{V}\right)$ with Ω the angular velocity of the Sun and θ , ϕ and r the heliocentric spatial coordinates. The solar wind speed V was assumed to change from 450 km.s⁻¹ in the equatorial plane ($\theta = 90^\circ$) to a maximum of 850 km.s⁻¹ when $\theta \leq 60^\circ$. The HMF was modified according to Jokipii & Kóta (1989) and the outer boundary of the simulated heliosphere was assumed at 100 AU. The galactic electron spectrum based on COMPTEL results (Strong et al., 1994) was assumed as the local interstellar spectrum.

To produce spectra compatible to both Ulysses and Voyager 1 measurements (Potgieter et al., SH3.1.06), the following parallel diffusion coefficient was used:

$$K_{\parallel} = \frac{v}{3} \beta r_0 \left[\left(\frac{P}{P_0} \right)^2 DE + \frac{(P/P_0)^{0.2}}{10} E + \left(1 + \frac{r}{10r_0} \right) \left(\left(\frac{r_0}{r} \right)^2 - \frac{1-r/r_0}{(r/r_0)^3} \right) GE \right]. \quad (2)$$

Here $D = \frac{(r/r_0)^{0.8} - 1}{20}$, $G = \left(5 - \frac{5}{e^F} \right)^2$ with $F = \frac{0.9}{P/P_0}$ and $E = 40 - \frac{r/r_0}{7 - r/(40r_0)} - (r/r_0)^{0.6}$,

and $P_0 = 1$ GV and $r_0 = 1$ AU. Assuming Eq. (2), and apart from the inherent azimuthal dependence of the HCS, no additional azimuthal dependence was incorporated in the 3D model. For the perpendicular diffusion and the “drift” coefficient the following general forms were assumed respectively:

$$K_{\perp r} = aK_{\parallel}; K_{\perp \theta} = bK_{\parallel}; K_A = (K_A)_0 \frac{\beta P}{3B_m} \quad (3)$$

Here β is the ratio of the speed of the CR particles to the speed of light, $a = 0.05$ is a constant determining the value of $K_{\perp r}$ which contributes to perpendicular diffusion in the radial direction; $b = 0.15$ is a constant determining the value of $K_{\perp \theta}$ which contributes to perpendicular diffusion in the polar direction. Diffusion perpendicular to the HMF was therefore enhanced in the polar direction by assuming $b > a$. (Kóta & Jokipii, 1995; Potgieter, 1996). $(K_A)_0$ specifies the amount of drifts allowed. For this work it was necessary to take $(K_A)_0 = 0.5$ which corresponds to medium drift effects; B_m is the magnitude of the modified HMF. The effective radial diffusion coefficient is given by $K_{rr} = K_{\parallel} \cos^2 \psi + K_{\perp r} \sin^2 \psi$, with ψ the angle between the radial direction and the averaged HMF direction. Note that $\psi \rightarrow 90^\circ$ when $r > \sim 10$ AU with the polar angle $\theta \rightarrow 90^\circ$, and $\psi \rightarrow 0^\circ$ when $\theta \rightarrow 0^\circ$, which means that K_{\parallel} dominates K_{rr} in the inner and polar regions and $K_{\perp r}$ dominates in the outer equatorial regions of the heliosphere. The differential intensity, $j \propto P^2 f$, is calculated in units of particles m⁻² sr⁻¹ s⁻¹ MeV⁻¹.

3 Results and Discussion

To compare the results of the 3D model with the 2D WCS model, the average of the 3D solutions had to be calculated over one solar rotation, i.e. for azimuthal angles $\phi = 0 \rightarrow 2\pi$. As a first comparison the modulated electron spectra computed with both models are shown in Figure 1a for the polar regions, $\theta = 30^\circ$, and in Figure 1b for the equatorial regions, $\theta = 90^\circ$, respectively at radial distances of 1 AU and 60 AU with $\alpha = 20^\circ$. Solutions are shown for the A > 0 polarity epoch (e.g. ~1990 to ~2000) only, because during this cycle when electrons are drifting in along the HCS the largest difference between the two models occurs; see discussion below. These spectra can be considered as typical for minimum modulation periods. Evidently, the electron spectra produced by the two models as shown in Figure 1 essentially coincide despite the use of a rather complex rigidity dependence for K_{\parallel} and K_{\perp} .

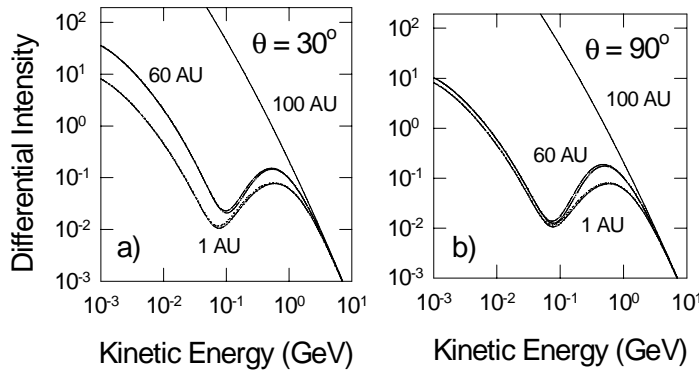


Figure 1. a) Computed electron spectra produced by the 2D and 3D drift model. Differential intensities are shown for 1 AU and 60 AU at a polar angle of $\theta = 30^\circ$ and a “tilt angle” of 20° in units of $\text{m}^{-2}\text{sr}^{-1}\text{s}^{-1}\text{MeV}^{-1}$ for the $A > 0$ polarity cycle. b) Similar, but for a polar angle of $\theta = 90^\circ$. Note that the spectra for the two models essentially coincide.

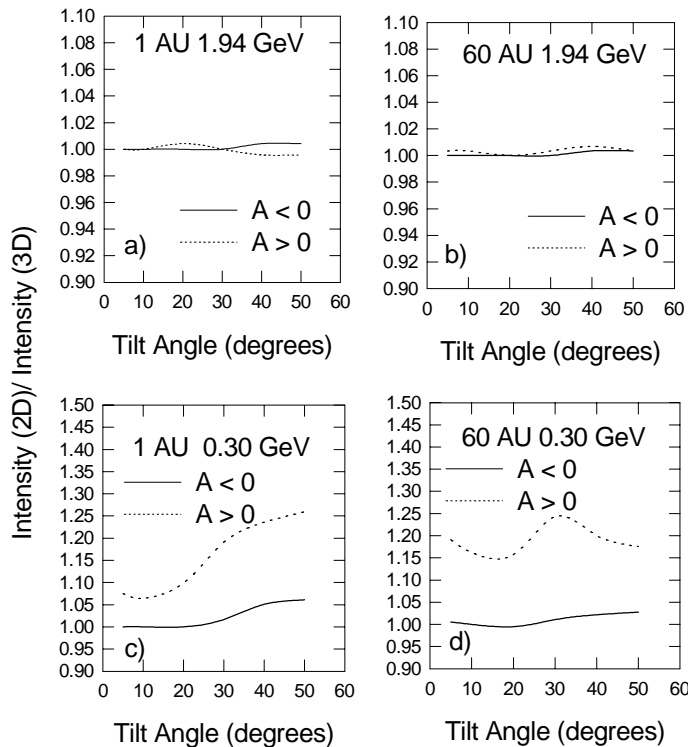


Figure 2. The ratio of electron differential intensities computed with the 2D and 3D drift models as a function of tilt angle. Panel a) shows the ratio for 1.94 GeV electrons for both the $A > 0$ and $A < 0$ polarity cycles at 1 AU and panel b) shows the situation at 60 AU. Panels c) and d) display the situation for 0.30 GeV electrons at 1 AU and 60 AU respectively.

The two models obviously differ in the way the HCS is treated. Therefore, an appropriate way to compare the two models is by examining the α dependence of the differential intensities. In Figure 2 the ratio of the computed 2D and 3D differential intensities is shown as a function of α for both the $A > 0$ and $A < 0$ magnetic polarity cycles. The modulation parameters are the same as for Figure 1. Values are shown for 1.94 GeV electrons at 1 AU in Figure 2a and at 60 AU in Figure 2b. Figures 2c and 2d show the same situation but for 0.30 GeV.

From this figure follows that for 1.94 GeV electrons the ratio varies with $< \sim 1\%$ for both polarity cycles, at 1 AU and at 60 AU, for all α 's. At 0.30 GeV, the $A < 0$ polarity cycle exhibits again a very small deviation from unity in the ratio, not more than $\sim 5\%$. For the $A > 0$ cycle, however, the ratio is > 1.0 at 1 AU, increasing with increasing α , with a maximum of 1.25. At 60 AU the ratio has a peculiar α dependence varying between 1.15 and 1.25 which is larger than at 1 AU, especially for $\alpha < \sim 30^\circ$.

The differences between the model solutions are obviously the largest for the intermediate to lower energies during the $A > 0$ cycle when the electrons drift in along the HCS. At energies below ~ 0.05 GeV the differences between the intensities dissipate quickly because electrons experience less and less drift effects with decreasing energy. The largest variation in the ratio between the two sets of solutions as a function of energy occurs at ~ 0.2 GeV and varies between 12% at 1 AU and 24% at 60 AU, with no difference at kinetic energies $> \sim 1$ GeV. No qualitative differences were found between the solutions of the two models despite the difference in spatial dimensions and the different way the HCS was handled in the numerical schemes.

Hattingh (1998) indicated that the difference in the solutions of the 2D and 3D models using the same set of modulation parameters was somewhat

dependent on the parameter values. The values used above correspond to solar minimum modulation conditions for which the steady-state models were developed. When more extreme variations were used the differences between the two models increased, indicating that some caution is required during periods of large modulation. Investigating this aspect further using electron modulation it was found that by increasing $K_{\perp 0}$, which has become a very important parameter in modulation models, a reduction in the differences between the 2D and 3D model solutions followed (see also e.g. Ferreira et al., SH3.1.14 and Ferreira & Potgieter, SH3.1.07). This is expected because an increasing $K_{\perp 0}$ causes less pronounced drift effects. It is worthwhile to mention that when no-drifts were used the two models produce identical solutions under all circumstances. Reducing the azimuthal, radial, polar and rigidity grid intervals, that is increasing the number of total grid points in the numerical scheme, resulted in only a slight reduction in the difference between the two models while the runtime in computing one solution increased considerably for the 3D model (Ferreira, 1999).

4 Conclusions

Comparing the solutions produced by the 2D and 3D numerical modulation models that were both developed by the Modulation Group in Potchefstroom, it was found that when examining electron spectra as a function of the HCS “tilt angle” α , no qualitative differences occurred between the two sets of solutions when using identical parameters. Quantitatively, in the inner heliosphere the ratio between the two sets of solutions increased with increasing α 's, with 25% the largest difference at intermediate energies (~ 0.30 GeV) for $\alpha > 30^\circ$ during the $A > 0$ cycle; at 60 AU the ratio varied with 15% to 25% with no clear trend in the α dependence of the intensities. At energies below ~ 0.05 GeV the differences between the intensities dissipate quickly because electrons experience diminishing drift effects with decreasing energy. For the $A < 0$ cycle, the solutions were essentially identical. Thus, with no qualitative differences and insignificant quantitative differences between the solutions of the 2D and 3D models, and taking into account the amount of computing time and resources needed for the 3D model, the use of the 2D drift model for modulation studies is still well justified.

References

- Burger, R. A., & Potgieter, M. S. 1989, ApJ 339, 501
Burger, R. A., & Hattingh, M. 1995, Astrophys. Space Sci 230, 375
Burger, R. A., & Hattingh, M. 1998, ApJ 505, 244
Hattingh, M., & Burger, R. A. 1995a, Adv. Space Res. 13(9), 9213
Hattingh, M., & Burger, R. A. 1995b, Proc. 24th ICRC (Roma) 4, 337
Hattingh, M. 1993, M.Sc. dissertation, Potchefstroom University for CHE, Potchefstroom. South Africa
Hattingh, M. 1998, Ph.D. thesis, Potchefstroom University for CHE, Potchefstroom. South Africa
Ferreira, S. E. S. 1999, M.Sc. dissertation, Potchefstroom University for CHE, Potchefstroom. South Africa
Jokipii, J. R., & Kóta, J. 1989, Geophys. Res. Let. 16, 1
Kóta, J., & Jokipii, J. R. 1983, ApJ 265, 573
Kóta, J., & Jokipii, J. R. 1995, Proc. 24th ICRC (Roma) 4, 680
le Roux, J. A., & Potgieter, M. S. 1990, ApJ 361, 275
Parker, E. N. 1965, Plan. Space Sci. 13, 9
Potgieter, M. S. 1996, J. Geophys. Res. 101, 24411
Potgieter, M. S. & Moraal, H. 1985, ApJ 294, 425
Strong A., et al. 1994, Astron. Astrophys. 292, 82